ELSEVIER

Polymer 42 (2001) 7477–7493

polymer

www.elsevier.nl/locate/polymer

A phenomenological study of the hot-tool welding of thermoplastics. 4. Weld strength data for several blends

Vijay K. Stokes*, Kenneth R. Conway

GE Corporate Research and Development, Engineering Mechanics Laboratory, P.O. Box 8, Building K1, Room 3A20, Schenectady, NY 12301, USA

Received 18 September 2000; received in revised form 10 February 2001; accepted 18 February 2001

Abstract

A hot-tool welding machine was used to study the hot-tool weldability of several commercial thermoplastic blends: a blend, ABS, of acrylonitrile–butadiene–styrene; a blend, PC/ABS, of polycarbonate (PC) and ABS; a blend, PC/PBT, of PC and poly(butylene terephthalate) (PBT); a blend, M-PPO, of poly(phenylene oxide) (PPO) and HIPS; a blend, PPO/PA, of PPO and polyamide 6,6; 30GF-MPPO, a 30 wt% glass-filled grade of M-PPO. Weld strength data are reported for a specimen thickness of 3.2 mm. In these experiments, the outflow in the melting phase was controlled by means of stops, the thickness of the molten film was controlled by the heating time, and the outflow during the final joining phase was also controlled by displacement stops. Strength data for butt welds are reported for a series of tests in which the hot-tool surface temperatures, the heating times, and the displacement stop positions were varied, but the pressure was not. The maximum relative weld strengths demonstrated are 100% in ABS, 91% in PC/ABS, 98% in PC/PBT, 80% in M-PPO, 100% in PPO/PA and 77% in 30GF-MPPO. A maximum relative strength of 38% was obtained in hot-tool welds of PC/ABS to M-PPO.

Keywords: Hot-tool welding; Thermoplastics; Blends

1. Introduction

Because of the increasing use of thermoplastics and thermoplastic composites in load-bearing applications, welding methods are becoming important for part cost reduction. Hot-tool welding is a widely used technique in which the surfaces to be joined are brought to the 'melting temperature' by direct contact with a heated metallic tool. In some cases, such as the joining of plastic pipes, the surfaces to be joined are flat, so that the tool is a hot plate. However, in many applications, such as in automotive headlamps and rear lights, doubly curved joint interfaces require complex tools that allow the hot surfaces to match the contours of the joint interface. Applicability to complex geometries is one of the major advantages of this process.

This paper is the fourth in a series dealing with the hot-tool welding of thermoplastics. The hot-tool welding process is described in detail in Part 1 of this paper, which presents a comprehensive phenomenological study of the hot-tool welding of the amorphous polymer BPA polycarbonate (PC) [1]. Part 2 addresses the weldability of unfilled and glass-filled poly(butylene terephthalate) (PBT) [2]. Part 3 discusses the weldability of polyetherimide (PEI), a high-temperature thermoplastic [3]. In addition to establishing the terminology, the first two parts include comprehensive lists of references on hot-tool welding, including those on the weldability of other thermoplastics. As such, in this paper, only papers pertinent to the study reported in this paper are cited.

This paper examines the hot-tool weldability of several commercial thermoplastic blends: a blend, ABS, of acrylonitrile–butadiene–styrene; a blend, PC/ABS, of PC and ABS; a blend, PC/PBT, of PC and PBT; a blend, M-PPO, of poly(phenylene oxide) (PPO) and HIPS; a blend, PPO/PA, of PPO and polyamide 6,6; 30GF-MPPO, a 30 wt% glass-filled grade of M-PPO. The effects of the large number of welding parameters were explored mainly by conducting one test per test condition studied; such data do not provide information on the variability in the weld strength at each test condition.

2. Displacement controlled welding

This process is described in detail in Ref. [1]. The essential parts of a displacement controlled welding machine consist of the hot-tool assembly having two exposed hot

* Corresponding author. Tel.: +1-518-387-5157; fax: +1-518-387-7006.
E-mail address: stokes@crd.ge.com (V.K. Stokes).

0032-3861/01/$ - see front matter
PII: S0032-3861(01)00182-3

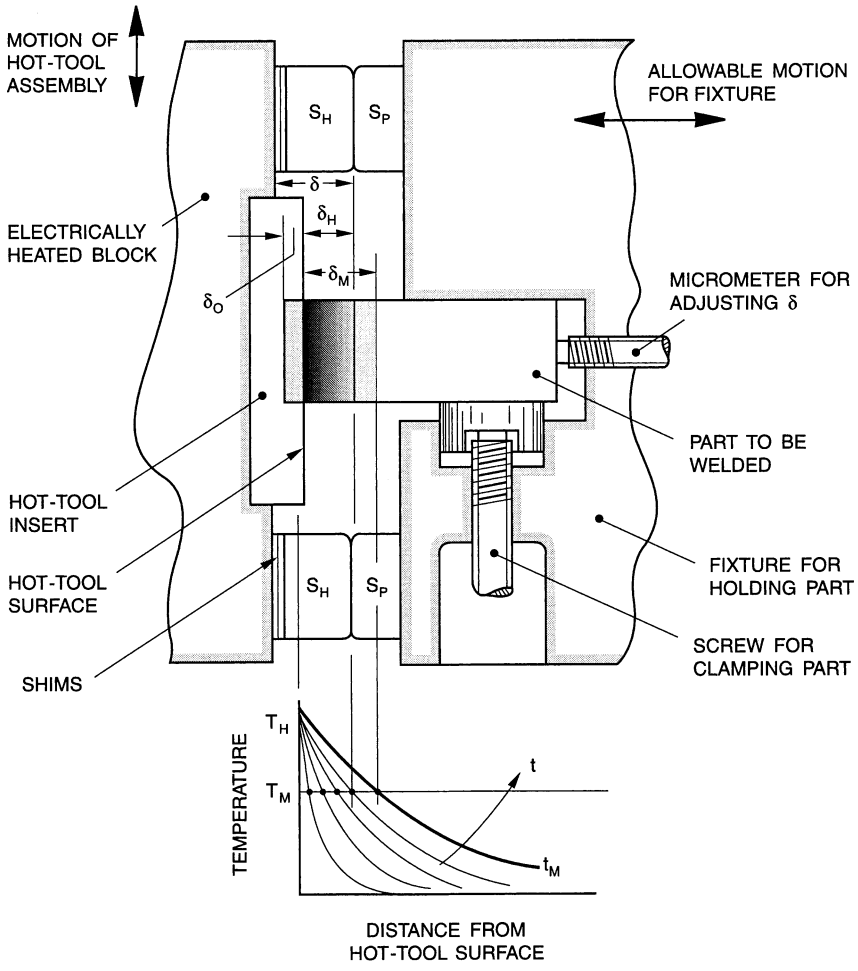

Fig. 1. Schematic diagram showing geometric parameters for displacement-controlled hot-tool welding using mechanical stops.

surfaces, two fixtures for holding the parts to be welded, means for bringing the parts in contact with the hot surfaces and then bringing the molten surfaces together to form the weld, and adequate timing and displacement controls. The mechanics of the hot-tool welding process using mechanical stops to effect displacement control can be described by means of the schematic in Fig. 1. The left-hand side shows one half of the hot-tool assembly, comprising an electrically heated block on which interchangeable hot-tool inserts can be mounted. The hot-tool assembly has mechanical stops S_H, the surfaces of which are offset from the hot-tool surface by a distance δ_H. The hot-tool assembly can be moved in and out of the configuration shown in the figure along the direction indicated.

The part to be welded is gripped in a fixture (right-hand side of figure) that can be moved to and fro in a direction at right angles to the allowable motion for the hot-tool assembly. This fixture has mechanical stops S_P that are aligned with the hot-tool stops S_H.

For welding, the fixture is moved to bring the part into contact with the hot-tool surface, and a pressure is applied to maintain this contact. Heat transfer raises the temperature of the part and the resulting thermal expansion causes a small rightward (away from the hot-tool surface) motion in the part and fixture. When the surface temperature reaches the melting point of the plastic, the externally applied pressure causes the molten material to flow laterally outward, thereby inducing a leftward motion of the part. The decrease in the part length caused by the outflow of molten material is called the penetration η, which for this phase is the part displacement from the instant of contact, and weld time is measured from this instant.

Initially, when the surface begins to melt, very little flow occurs and the molten film thickens. The flow or penetration rate begins to increase with time. The penetration (or part motion) will not change after the part stops S_P come into contact with the hot-tool stops S_H, as shown in Fig. 1. Let the elapsed time from the instant that the part touches the hot-tool surface to the instant when the stops come into contact be t_0, and let the corresponding penetration, the melt penetration, be $\eta = \delta_0$ (Fig. 1).

This thickness of material will melt and flow out laterally to form a part of the weld 'bead'. Continuing contact with the hot-tool surface after time t_0 will cause the molten layer to thicken with time. During this phase, there will be no additional penetration. However, with increasing time,

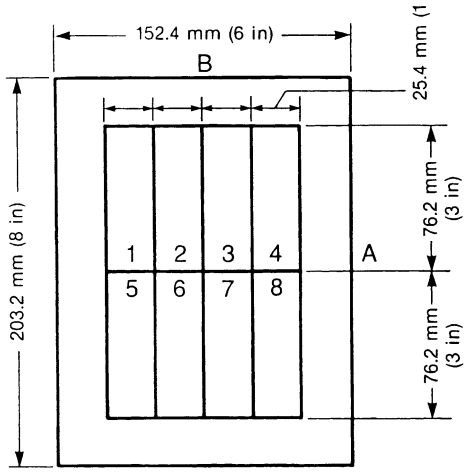

Fig. 2. Layout showing the locations of eight numbered specimens cut from 152 mm × 203 mm injection-molded plaques.

thermal expansion in the portion of the part heated by conduction will cause more material to flow out, thereby resulting in an apparent increase in δ_0. Let the duration of this film buildup phase be t_M and let the thickness of the molten layer be δ_M as shown. In the changeover phase, the parts are pulled away from the hot-tool, the hot-tool is retracted, and the molten surfaces are brought into contact — thereby initiating the joining phase. Let the duration of this changeover phase be t_c. After the molten surfaces touch, the applied joining pressure squeezes out the molten material laterally, resulting in a further penetration. During this squeezing motion, heat transfer from the melt results in a cooling and in an eventual solidification of the melt.

Two possible cases are important. If $\delta_M < \delta_H$, the part stops S_P cannot come into contact, so that part dimensions cannot be controlled. However, if $\delta_M > \delta_H$, the material in the molten layer will continue to be squeezed out until the stops S_P come into contact, after which part motion will stop and the melt will solidify without further motion. For dimensional control, t_M should be large enough to ensure that $\delta_M > \delta_H$. For this case, the total penetration on each of the halves being welded will be $\delta = \delta_0 + \delta_H$ so that the overall (warm) part length will decrease by 2δ, if thermal expansion effects are neglected. Let the initial lengths of the parts before welding be l_1 and l_2, and let the length of the welded part be l_0. Then, $\Delta l = l_1 + l_2 - l_0$ is the thickness of the material that flowed out into the weld bead. If the stops come into contact during the joining phase (for which $\delta_M > \delta_H$) and thermal expansion effects are neglected, then the expected change in length should be 2δ. However, if $\delta_M < \delta_H$, then the stops will not come into contact and the change in length should be less than 2δ. Thus, if thermal expansion effects are neglected, $\Delta\eta = 2\delta - \Delta l$ is a measure for whether or not the stops come into contact: stops do and do not contact when $\Delta\eta = 0$ and $\Delta\eta > 0$, respectively. However, thermal expansion at the heated ends of the specimens would increase Δl and, in the case in which stops contact, could result in negative values of the differential penetration $\Delta\eta$. Thus, a larger Δl could result from thermal expansions both in Phase 1 (an apparent increase in δ_0) and during the joining phase. Let the thermal expansion of the specimen be δ_T, so that the effective change in length would be $2(\delta + \delta_T)$. Then, $\Delta\eta_T = 2(\delta + \delta_T) - \Delta l = \Delta\eta + 2\delta_T$ will be a better measure for whether or not stops come into contact.

Estimates [1] for this temperature-induced length increase, δ_T, have been used to estimate $\Delta\eta_T$ for PC [1], PBT [2] and PEI [3]. However, the use of this correction did not provide a significantly better measure for whether or not the stops come into contact. One explanation for this lack in improvement could be errors in the measurements of δ_0 and the weld penetration δ_H. Because $\Delta\eta_T$ did not provide a better measure, in this paper, only $\Delta\eta$ is tabulated for the different blends studied.

As the molten material cools, thermal contraction generates tensile stress in the solidifying material. This stress field can affect the residual stresses induced by the nonhomogeneous cooling. Clearly, δ_0 by itself does not contribute to the welding that occurs during the joining phase; this material just flows outward into the bead. A small value of δ_0 is required to compensate for part surface irregularities and for ensuring that contaminated surface layers flow out before the joining phase. The weld penetration, the penetration $\eta_j = \delta_H$ during the joining phase, is controlled by the machine setting δ_H (Fig. 1). Let the duration of the joining (or welding) phase, from the instant the molten surfaces touch to the instant the solidified weld is released, be t_w. Then the total welding time is given by $t_T = t_0 + t_M + t_c + t_w$. Clearly, t_c should be as small as possible.

In this paper, the total time $t_H = t_0 + t_M \approx t_M$ for which the specimen is in contact with the hot-tool will be referred to as the heating time; melt penetration will refer to the distance δ_0 (Fig. 1); weld penetration will refer to the distance δ_H; the time t_w will be referred to as the seal time.

3. Test procedure

All the test data in this paper were obtained from 3.2 mm-thick specimens cut from 152 mm × 203 mm injection molded plaques of Cycolac® BDT 6500, a blend, ABS, of acrylonitrile–butadiene–styrene; Cycoloy® C2950HF, a blend, PC/ABS, of PC and ABS; Cycoloy® MC8002, a slightly different blend of PC and ABS; Xenoy® 1102, a blend, PC/PBT, of PC and PBT; Noryl® EM6100, a blend, M-PPO, of PPO and HIPS; Noryl® GTX910, a blend, PPO/PA, of PPO and polyamide 6,6; Noryl® GFN3 (30GF-MPPO), a 30 wt% glass-filled grade of M-PPO. The edges of each specimen were machined to obtain rectangular blocks of size 76.2 mm × 25.4 mm × thickness for assuring accurate alignment of the surfaces during butt welding along the 25.4 mm × thickness edges.

For the glass-filled material, 30GF-MPPO, eight specimens

were cut from the 152 mm × 203 mm injection molded plaques that were gated at the 152 mm edge (gate B in Fig. 2), as per the layout shown in Fig. 2. The specimens were individually numbered according to the scheme shown in Fig. 2 [2,4]. Welds were conducted on sets of mating specimens from the same plaque. In this way, it was possible to track variations across plaques due to fiber orientation. Fiber orientation in the specimens, which depends both on the location in the specimen as well as on its thickness, was not characterized. However, for purposes of comparison, four 152 mm × 25 mm specimens, corresponding to locations 1–4 in Fig. 2, were cut from the 152 mm × 203 mm plaques. These specimens were subjected to the same strength tests as the welded specimens, thereby providing a basis for evaluating the strengths of the welded joints.

All the welds were made on a commercially available (Hydra-Sealer Model VA-1015, Forward Technology Industries) dual platen hot-tool welding machine in which the temperatures of the two hot-tool surfaces can be independently controlled. On this machine, the offset δ_H, called the weld penetration, of the hot-tool stop S_H from the hot-tool surface (Fig. 1) can only be changed by inserting shims between the electrically heated hot-tool block and the stops, which are fastened to the block surface by means of screws. All the data in this paper were obtained at a fixed melt penetration of $\delta_0 = 0.13$ mm and two weld penetrations of $\delta_H = 0.25$ and 0.66 mm. For M-PPO, additional data were acquired at a weld penetration $\delta_H = 0.91$ mm.

The weld specimens are pneumatically gripped in special fixtures that accurately align the specimens during the welding cycle. Each grip is provided with a micrometer that can be used to accurately set the distance δ by which each specimen protrudes beyond the stops S_P; any variations in the lengths of the specimens can easily be compensated for. In this machine, the times t_0 and t_M cannot be resolved, only the total heating time $t_H = t_0 + t_M$ can be set and measured. However, for $\delta_0 \ll \delta_H$ should be much smaller than t_M. The changeover time t_c, from the instant the heated specimens are pulled back from the hot-tool to the instant the molten films are brought back into contact, can be changed by changing the decelerating springs and the air pressure on the displacement pistons. However, the possible range of variation is quite small. In the tests reported in this paper, a fixed changeover time t_c of about 1.24 s was used; the corresponding average changeover velocity seen by the specimen molten surfaces was about 118 mm s^{-1}. The welding, or joining, time t_w — measured from the instant the molten films are brought into contact to the instant the (solidified) welded parts are released — can be preset for on this machine.

One limitation of this machine is the lack of adequate pressure control at the weld interface. For the 3.2 mm-thick welds (specimen cross-sections of thickness × 25.4 mm), the nominal weld pressure (based on the air pressure and the piston cross-sectional area) was 6.9 MPa.

An important characteristic of the hot-tool surface is the extent to which molten polymer tends to stick to the surface. Residue left behind can affect the quality of subsequent welds: First, because of the high temperature, the accumulated material can degrade, transfer to subsequent welds, and act as an inclusion. Second, the accumulated layer can affect heat transfer, and third, the texture of the surface residue can affect the geometry of the molten part surface. To reduce this tendency for sticking, the surface of the hot-tool insert can be coated with a non-stick coating, such as Teflon®; an alternative is to cover the hot-tool surface with a thin Teflon cloth. However, Teflon coatings and cloth can only be used up to hot-tool temperatures of about $T_H = 260°C$. Because hot-tool temperatures as high as 380°C were used, an uncoated metal insert, made of a high-conductivity copper–nickel–silicon–chromium alloy (Ampco 940, about 96% of which is copper), was used for all the tests reported in this paper. To eliminate the effects of residues resulting from the tendency of the melt to stick to the surface, a copper scraper was used to clean the hot-tool surface after each test.

In contrast to the weld studies on PC and PBT [1,2], the textures of the melt surfaces just before the final joining phase, which can be expected to affect weld quality, were not studied.

The test procedure for determining weld strength is as follows: First, the hot-tool surfaces are allowed to attain the desired surface temperatures. After accurately measuring their lengths, the weld specimens are mounted on the specimen holding fixtures and the micrometer settings are adjusted to obtain desired values of the overhang δ. The heating time t_H and the welding time t_w are set and the machine is cycled to effect the weld. The weld results in a 152.4 mm × 25.4 mm × thickness bar. After sufficient cooling, the length of the bar is accurately measured with a micrometer. The difference Δl of this final length from the combined lengths of the unwelded specimen pairs determines the thickness of the material that actually flowed out, i.e. the actual penetration, which can be compared with 2δ. The rectangular bar is routed down to a standard ASTM D638 tensile test specimen with a butt joint at its center [5]. The tensile bar, which has a transverse butt weld at mid-length, is then subjected to a constant displacement rate tensile test in which the strain across the weld is monitored with an extensometer. In this way, the average failure strain across the weld over a 25.4 mm gauge length can be monitored. All the weld strength tensile tests reported in this paper were done at a nominal strain rate of 0.01 s^{-1}.

The weld flash, or 'bead,' was not removed, and the weld strengths were obtained by dividing the load at failure by the original cross-sectional area of the specimen. Because large local deformations at the weld interface increase the local cross-sectional area, the true failure stress (based on the actual local cross-sectional area) will be smaller than the nominal stress (based on the original cross-sectional area) reported in this paper [6].

Furthermore, the 25.4 mm gauge-length extensometer can grossly underestimate the local strain in the failure

Table 1
Strength and ductility data for hot-tool welds of 3.2 mm-thick ABS (Cycolac BDT 6500) specimens, at a strain rate of $\dot{\varepsilon} = 0.01\ s^{-1}$, as functions of the hot-tool temperature and the heating time, for two weld penetrations of 0.25 and 0.66 mm. The melt penetration was maintained at 0.13 mm and the seal time was kept constant at 10 s

Hot-tool temperature (°C)	Heating time (s)	Weld strength (MPa)		Relative weld strength[a] (%)		Failure strain[b] (%)		Δl (mm)		Differential penetration $\Delta\eta$ (10^{-2} mm)	
		$\delta_H = 0.25$ mm	$\delta_H = 0.66$ mm	$\delta_H = 0.25$ mm	$\delta_H = 0.66$ mm	$\delta_H = 0.25$ mm	$\delta_H = 0.66$ mm	$\delta_H = 0.25$ mm	$\delta_H = 0.66$ mm	$\delta_H = 0.25$ mm	$\delta_H = 0.66$ mm
155	10	11.3	–	30	–	0.48	–	0.80	–	−4	–
170	10	13.9	11.5	37	30	0.61	0.48	0.91	1.34	−15	24
185	10	16.4	14.7	43	39	0.74	0.62	0.90	1.43	−14	15
200	10	18.0	22.7	47	60	0.81	0.99	0.93	1.46	−17	12
215	10	20.7	31.1	55	82	0.93	1.44	1.01	1.42	−25	16
230	10	14.7	37.8	39	100	0.66	2.16	1.05	1.43	−29	15
245	10	25.3	37.7[c]	67	100	1.20	2.15	0.96	1.47	−20	11
260	10	15.6	39.0	41	103	0.73	2.12	1.05	1.46	−29	12
275	10	–	37.0	–	98	–	1.90	–	1.51	–	7
155	15	11.7	–	31	–	0.50	–	0.88	–	−12	–
170	15	15.2	14.4	40	38	0.67	0.63	0.94	1.41	−18	17
185	15	17.5	21.1	46	56	0.80	0.94	0.89	1.42	−13	16
200	15	24.2	30.0	64	79	1.17	1.39	0.94	1.38	−18	20
215	15	19.9	36.8	53	97	0.95	1.82	0.96	1.42	−20	16
230	15	16.7	38.1[c]	44	100	0.78	2.21	1.04	1.44	−28	14
245	15	15.7	37.7	41	100	0.76	2.20	0.96	1.48	−20	10
260	15	9.2	36.5	24	96	0.43	1.86	1.08	1.53	−32	5
275	15	–	12.0	–	32	–	0.59	–	1.59	–	−1
155	20	10.8	–	29	–	0.44	–	0.91	–	−15	–
170	20	21.9	15.7	58	41	1.00	0.68	0.89	1.40	−13	18
185	20	19.3	24.0	51	63	0.90	1.06	0.89	1.37	−13	21
200	20	25.4	27.3	67	72	1.20	1.30	0.93	1.36	−17	22
215	20	15.0	35.4	40	93	0.68	1.73	0.99	1.46	−23	12
230	20	11.0	37.1	29	98	0.49	2.22	1.04	1.46	−28	12
245	20	12.1	30.4	32	80	0.61	1.54	1.06	1.49	−30	9
260	20	11.0	33.6	29	89	0.48	1.73	1.10	1.54	−34	4
275	20	–	18.9	–	50	–	0.90	–	1.67	–	−9

[a] Based on a resin strength of $\sigma_0 = 37.9$ MPa.
[b] $\varepsilon_0 = 2.25\%$.
[c] Specimen failed outside the weld.

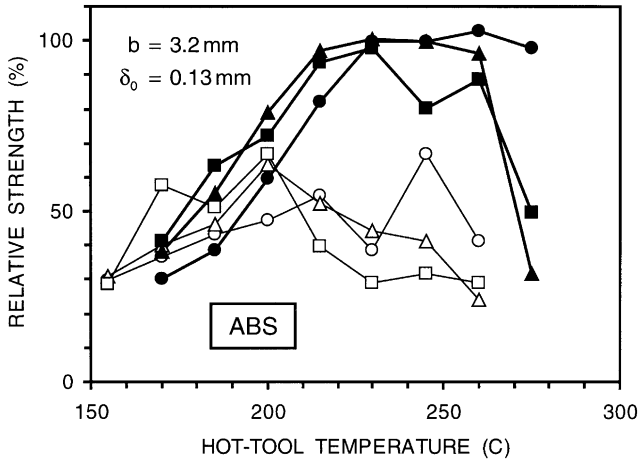

Fig. 3. Weld strength of 3.2 mm-thick ABS as a function of the hot-tool temperature, with the heating time as parameter. Circles, triangles and squares correspond, respectively, to heating times of 10, 15 and 20 s. Open symbols (connected by thin lines) and solid symbols (connected by thick lines) correspond to weld penetrations of 0.25 and 0.66 mm, respectively. The melt penetration was maintained at 0.13 mm and the seal time was 10 s.

region once strain localization sets in, so that the significance of the reported failure strains ε_0 should be interpreted with care. These values only represent the lower limit of the failure strain at the weld.

4. Weld strength of ABS (Cycolac BDT 6500)

Welds of 3.2 mm-thick ABS specimens, having a yield strength of 37.9 MPa and a yield strain of 2.25%, were made at the following conditions: Hot-tool temperatures from $T_H = 155$ to 275°C, heating times of $t_H = 10$, 15 and 20 s, a melt penetration of $\delta_0 = 0.13$ mm, two weld penetrations of $\delta_H = 0.25$ and 0.66 mm and a seal time of $t_w = 10$ s. Strength and ductility data at a nominal strain rate of 0.01 s^{-1}, and differential penetration data for welds made at these conditions, are listed in Table 1. In this table, columns 5 and 6 list, respectively, the relative weld strengths (weld strength/strength of ABS resin), based on an ABS resin strength of 37.9 MPa, obtained at weld penetrations of 0.25 and 0.66 mm.

The open symbols in Fig. 3, connected by thin lines, show the relative weld strength (data from Table 1) for a weld penetration of 0.25 mm as a function of the hot-tool temperature in the temperature range of $T_H = 155$–260°C, for three heating times of 10, 15 and 20 s (indicated, respectively, by open circles, triangles and squares). For a heating time of $t_H = 10$ s, relative weld strengths lie in the range 30–67%; the maximum relative strength of 67% is obtained at $T_H = 245$°C. The corresponding failure strains are in the range 0.48–1.20%. For $t_H = 15$ s, relative weld strengths ranging from 24 to 64% are obtained, with the maximum of 64% occurring at $T_H = 200$°C; the failure strains are in the range 0.43–1.17%. For $t_H = 20$ s, relative weld strengths range from 29 to 67%, with the maximum of 67% occurring at $T_H = 200$°C; the failure strains are in the range 0.44–1.20%. Thus, for a weld penetration of 0.25 mm, relative strengths of about 67% can be attained over a hot-tool temperature window of 200–245°C for heating times of 10 and 20 s.

The filled symbols in Fig. 3, connected by thick lines, show the weld strength (data from Table 1) for the higher weld penetration of 0.66 mm as a function of the hot-tool temperature for three heating times of 10, 15 and 20 s (indicated, respectively, by filled circles, triangles and squares). For a heating time of $t_H = 10$ s, 100% relative weld strengths, with strains to failure of about 2.1%, can be obtained in the hot-tool temperature range $T_H =$ 230–260°C. A lower strength of 98%, with a strain to failure of 1.9% was obtained at $T_H = 275$°C. For $t_H = 15$ s, 100% relative weld strengths can be obtained for $T_H =$ 230–245°C, with failure strains of 2.2%. For $t_H = 20$ s, the highest relative weld strength of 98%, with a strain to failure of 2.2%, was obtained at $T_H = 230$°C. Thus, for a weld penetration of 0.66 mm, 100% relative strengths can be attained over a hot-tool temperature window of 230–245°C for $t_H = 10$ and 15 s.

Clearly, the highest weld strengths are obtained at the higher weld penetration of 0.66 mm, for which relative strengths in the range of 98–100% can be obtained in the temperature range of 230–275°C. For the lower weld penetration of 0.25 mm, the maximum weld strength obtainable was 67%.

Earlier, it was argued that, if thermal expansion effects are neglected, then the differential penetration $\Delta\eta \geq 0$, and that stops do and do not contact when $\Delta\eta = 0$ and $\Delta\eta > 0$, respectively. However, when thermal expansion at the heated ends of the specimens is accounted for, a better measure for whether or not stops come into contact is $\Delta\eta_T = \Delta\eta + 2\delta_T \geq 0$. The second-last column (data for the smaller weld penetration of 0.25 mm) in Table 1 shows that $\Delta\eta$ has negative values for all the test conditions shown. However, except for two test conditions, $\Delta\eta$ has positive values for the larger weld penetration of 0.66 mm (last column). Thus, for the higher weld penetration of 0.66 mm, the stops do not come in contact, and the melt apparently solidifies under pressure.

One explanation for the negative values of $\Delta\eta$ is that $\Delta\eta \geq 0$ really applies to $\Delta\eta_T = \Delta\eta + 2\delta_T$, and $\Delta\eta$ can be negative. However, another reason for such negative values can be errors in the measurements of δ_0 and the weld penetration δ_H. Instead of the two stops shown in the schematic in Fig. 1, contact is actually determined by four stops on each side. The difficulty in establishing even contact among the four stops on each side could result in errors in δ_0 and δ_H. A combined small increase of $\delta = \delta_0 + \delta_H = 0.25$ mm would make most values of $\Delta\eta$ in Table 1 positive [1–3].

Table 2
Strength and ductility data for hot-tool welds of 3.2 mm-thick PC/ABS-1 (Cycoloy C2950HF) specimens, at a strain rate of $\dot{\varepsilon} = 0.01\ s^{-1}$, as functions of the hot-tool temperature and the heating time, for two weld penetrations of 0.25 and 0.66 mm. The melt penetration was maintained at 0.13 mm

Hot-tool temperature (°C)	Heating time (s)	Seal time (s)		Weld strength (MPa)		Relative weld strength[a] (%)		Failure strain[b] (%)		Δl (mm)		Differential penetration $\Delta\eta$ (10^{-2} mm)	
		$\delta_H = 0.25$ mm	$\delta_H = 0.66$ mm	$\delta_H = 0.25$ mm	$\delta_H = 0.66$ mm	$\delta_H = 0.25$ mm	$\delta_H = 0.66$ mm	$\delta_H = 0.25$ mm	$\delta_H = 0.66$ mm	$\delta_H = 0.25$ mm	$\delta_H = 0.66$ mm	$\delta_H = 0.25$ mm	$\delta_H = 0.66$ mm
200	10	10	10	14.9[c]	35.1[c]	24	56	0.54	1.32	0.89	1.57	−13	1
215	10	10	10	28.3	41.8	45	66	1.08	1.54	0.91	1.64	−15	−6
230	10	10	10	34.0	41.3[c]	54	65	1.30	–[d]	0.98	1.64	−22	−6
245	10	10	10	48.9	48.6[c]	78	77	2.18	2.26[d]	1.03	1.68	−27	−10
260	10	10	10	46.9	47.1	74	75	2.16	2.18[d]	1.01	1.74	−25	−16
275	10	10	10	45.4	52.0	72	82	1.99	2.48[d]	1.02	1.79	−26	−21
290	10	10	10	50.8	57.3	81	91	2.44	2.61	1.05	1.69	−29	−11
305	10	10	10	54.6	48.1	87	76	2.79	1.98	1.15	1.84	−39	−26
320	10	–	10	–	55.8	–	89	–	2.59	–	1.82	–	−24
335	10	–	20	–	47.7	–	76	–	2.08	–	1.82	–	−24
350	10	–	20	–	50.2	–	80	–	2.39	–	1.85	–	−27
365	10	–	20	–	46.0[e]	–	73	–	2.08	–	1.82	–	−24
200	15	10	10	17.8[c]	31.6[c]	28	50	0.63	1.25	1.00	1.64	−24	−6
215	15	10	10	32.7	37.1	52	59	1.32	1.34	0.95	1.64	−19	−6
230	15	10	10	34.5	33.8[c]	55	54	1.39	–	0.98	1.64	−22	−6
245	15	10	10	51.2	37.5	81	60	2.48	1.66[d]	1.07	1.70	−31	−12
260	15	10	10	40.3	47.2	64	75	1.61	2.2[d]	1.02	1.73	−26	−15
275	15	10	10	40.2	52.8	64	84	1.79	3.09[d]	1.03	1.83	−27	−25
290	15	10	10	43.2	51.6	69	82	2.02	2.08[d]	1.04	1.79	−28	−21
305	15	10	10	50.7	52.7	80	84	2.38	2.47	1.22	1.79	−46	−21
320	15	–	10	–	52.1[e]	–	83	–	2.20	–	1.88	–	−30
335	15	–	20	–	50.0	–	79	–	2.34	–	1.84	–	−26
350	15	–	20	–	47.8[e]	–	76	–	2.00	–	1.85	–	−27
365	15	–	20	–	50.5[e]	–	80	–	2.32	–	1.92	–	−34
200	20	10	10	21.4[c]	25.4	34	40	0.80	0.90	1.00	1.60	−24	−2
215	20	10	10	30.4	29.9	48	48	1.18	1.00	0.97	1.65	−21	−7
230	20	10	10	36.0	33.5[c]	57	53	1.62	1.46[d]	1.03	1.65	−27	−7
245	20	10	10	46.4	48.0	74	76	2.12	2.27[d]	1.03	1.77	−27	−19
260	20	10	10	43.5	52.2	69	83	1.99	3.24[d]	1.04	1.75	−28	−17
275	20	10	10	48.3	56.2	77	89	2.20	3.53[d]	1.06	1.80	−30	−22
290	20	10	10	51.2	43.6	81	69	2.14	1.78	1.82	1.73	−106	−15
305	20	10	10	54.6	46.8	87	74	2.44	2.12	1.94	1.75	−118	−17
320	20	–	10	–	45.9[e]	–	73	–	1.83	–	1.87	–	−29
335	20	–	10	–	40.5[e]	–	64	–	1.64	–	1.94	–	−36
350	20	–	20	–	46.2[e]	–	73	–	1.98	–	1.89	–	−31
365	20	–	20	–	44.0[e]	–	70	–	1.90	–	2.41	–	−83

[a] Based on a resin strength of $\sigma_0 = 63.0$ MPa.
[b] $\varepsilon_0 = 4.42\%$.
[c] Failure surfaces had debris picked up from the hot-tool surfaces.
[d] 12.7 mm gauge-length extensometer used. Other specimens tested using a 25.4 mm gauge-length extensometer.
[e] Specimens sagged during the joining phase.

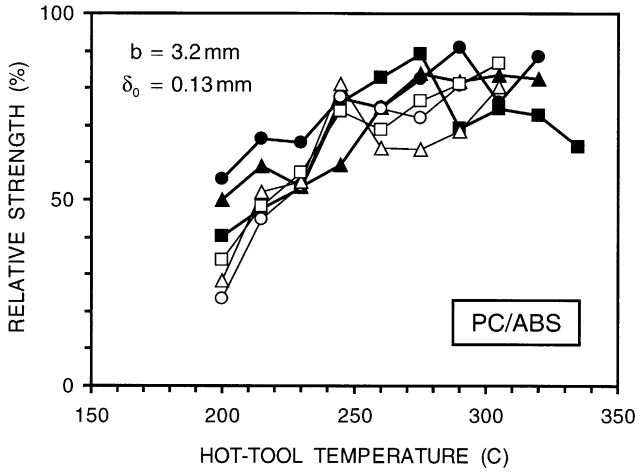

Fig. 4. Weld strength of 3.2 mm-thick PC/ABS-1 as a function of the hot-tool temperature, with the heating time as parameter. Circles, triangles, and squares correspond, respectively, to heating times of 10, 15 and 20 s. Open symbols (connected by thin lines) and solid symbols (connected by thick lines) correspond to weld penetrations of 0.25 and 0.66 mm, respectively. The melt penetration was maintained at 0.13 mm and the seal time was 10 s.

5. Weld strength of PC/ABS-1 (Cycoloy C2950HF)

Welds of 3.2 mm-thick PC/ABS-1 specimens, which had a yield strength of 63.0 MPa and a yield strain of 4.42%, were made at the following conditions: Hot-tool temperatures from $T_H = 200$ to 365°C, heating times of $t_H = 10$, 15 and 20 s, a melt penetration of $\delta_0 = 0.13$ mm and two weld penetrations of $\delta_H = 0.25$ and 0.66 mm. A seal time of $t_w =$ 10 s was used for $\delta_H = 0.25$ mm; two seal times of 10 and 20 s were used for $\delta_H = 0.66$ mm. Strength and ductility data at a nominal strain rate of 0.01 s^{-1}, and differential penetration data for welds made at these conditions, are listed in Table 2. In this table, columns 7 and 8 list, respectively, the relative weld strengths (weld strength/strength of PC/ABS resin), based on a PC/ABS resin strength of 63.0 MPa, obtained at weld penetrations of 0.25 and 0.66 mm.

The open symbols in Fig. 4, connected by thin lines, show the relative weld strength (data from Table 2) for a weld penetration of 0.25 mm as a function of the hot-tool temperature in the temperature range of $T_H = 200$–305°C, for three heating times of 10, 15 and 20 s (indicated, respectively, by the open circles, triangles and squares). For a heating time of $t_H = 10$ s, the relative weld strength increases rapidly with the temperature to about $\sigma_R = 78\%$ at $T_H = 245$°C, drops down at $T_H = 260$–275°C, and then increases to 81 and 87% at $T_H = 290$ and 305°C, respectively, the corresponding failure strains being 2.4 and 2.8%. The data for $t_H = 20$ s are very close to those for $t_H = 10$ s — the strengths at $T_H = 290$ and 305°C are the same at these two heating times, though the failure strains are a little lower at the higher heating time. For $t_H = 15$ s, except for a high $\sigma_R = 81\%$ measured at $T_H = 245$°C, σ_R is lower at higher temperatures for $t_H = 10$ and 20 s.

The filled symbols in Fig. 4, connected by thick lines, show the weld strength (data from Table 2) for the higher weld penetration of 0.66 mm as a function of the hot-tool temperature for three heating times of 10, 15 and 20 s (indicated, respectively, by the filled circles, triangles and squares). For a heating time of $t_H = 10$ s, the relative weld strength increases with the temperature to about $\sigma_R = 91$ and 89% at $T_H = 290$ and 320°C, respectively, with failure strains of about 2.6%. The relative strength drops down to 73% at $T_H = 365$°C. For $t_H = 15$ s, relative weld strengths in the range of 82–84%, with failure strains in the range of 2.1–3.1%, can be obtained over the fairly large temperatures range of $T_H = 275$–305°C. For $t_H = 20$ s, the highest relative strength of 89%, with a failure strain of about 3.5% is obtained at $T_H = 275$°C.

Clearly, with a maximum σ_R of about 91%, the relative weld strength for the higher weld penetration is higher than for the lower weld penetration of 0.25 mm. However, the differences between the weld strengths for the two weld penetrations are much smaller than those observed in ABS. Also, at the lower penetration, the weld strength appears to continue to increase with the temperature; it is possible that higher strengths could be obtained in the temperature range $T_H = 320$–365°C, in which tests were not done.

For both weld penetrations: (1) for $T_H \leq 170$°C, the failure surfaces had debris picked up from the hot-tool surfaces during the melting phase and (2) for $T_H \geq 215$°C, the molten surfaces smoked while being pulled away from the hot-tool surfaces during the change over phase. The strongest specimens exhibited 'stress whitening' at the weld interface. At very high weld temperatures, the weld failure surfaces were glossy.

5.1. Comparison with vibration welds

The vibration welding of a different batch of this material is discussed in Ref. [7], where a relative weld strength of 73%, with a failure strain of 1.8%, has been demonstrated for 3.2 mm-thick material that had a tensile strength of 59.8 MPa. Two things must be considered while comparing this value with the 91% relative weld strength obtained in hot-tool welds. First, this was a different batch of material, having a lower tensile strength (59.8 versus 63.0 MPa). Second, the strength of hot-tool welds reported can be higher than the true strength because of increased cross-sectional area at the weld interface [6]. Note that the highly laminated surface morphology in injection molded parts made of this materials results in a thickness dependence of weld strength; the vibration weld strength of 6.1 mm-thick specimens of this material, having a tensile strength of 64 MPa, was 84% with a failure strain of 2.3%. The overall effect of this laminated morphology is more noticeable in thinner specimens.

Table 3
Strength and ductility data for hot-tool welds of 3.2 mm-thick PC/PBT (Xenoy 1102) specimens, at a strain rate of $\dot{\varepsilon} = 0.01\ s^{-1}$, as functions of the hot-tool temperature and the heating time, for two weld penetrations of 0.25 and 0.66 mm. The melt penetration was maintained at 0.13 mm

Hot-tool temperature (°C)	Heating time (s)	Weld strength (MPa)		Relative weld strength[a] (%)		Failure strain[b] (%)		Δl (mm)		Differential penetration $\Delta\eta$ (10^{-2} mm)	
		$\delta_H = 0.25$ mm	$\delta_H = 0.66$ mm	$\delta_H = 0.25$ mm	$\delta_H = 0.66$ mm	$\delta_H = 0.25$ mm	$\delta_H = 0.66$ mm	$\delta_H = 0.25$ mm	$\delta_H = 0.66$ mm	$\delta_H = 0.25$ mm	$\delta_H = 0.66$ mm
200	10	–	–	–	–	–	–	–	–	–	–
215	10	15.7	18.6	29	34	0.80	–	0.74	1.13	2	45
230	10	41.8	48.1	76	88	2.47	3.00	0.87	1.42	−11	16
245	10	45.1	50.5	82	92	2.93	3.47	0.91	1.54	−15	4
260	10	45.5	51.8	83	95	2.91	4.03	1.03	1.61	−27	−3
275	10	37.2	52.9[c]	68	96	2.27	4.22	1.07	1.70	−31	−12
290	10	31.2	51.9[c]	57	95	1.92	4.25	1.09	1.60	−33	−2
305	10	–	51.7[d]	–	94	–	4.64	–	1.71	–	−13
320	10	–	53.9[c]	–	98	–	4.20	–	1.75	–	−17
335	10	–	52.9[c]	–	97	–	4.54	–	1.78	–	−20
350	10	–	49.9	–	91	–	3.49	–	1.77	–	−19
365	10	–	44.7	–	82	–	2.81	–	1.88	–	−30
200	15	5.7	9.8	10	18	0.26	0.46	0.65	1.08	11	50
215	15	17.2	22.5	31	41	0.87	1.10	0.82	1.32	−6	26
230	15	39.7	51.3[d]	72	94	2.27	3.88	0.94	1.51	−18	7
245	15	44.3	52.6[d]	81	96	2.73	4.37	0.97	1.59	−21	−1
260	15	37.0	53.1[d]	67	97	2.25	4.49	1.08	1.69	−32	−11
275	15	33.3	52.6[d]	61	96	2.03	4.35	1.11	1.70	−35	−12
290	15	26.4	53.5[d]	48	98	1.68	4.71	1.11	1.64	−35	−6
305	15	–	50.6	–	92	–	3.69	–	1.82	–	−24
320	15	–	46.6	–	85	–	3.05	–	1.78	–	−20
335	15	–	43.3	–	79	–	2.69	–	1.80	–	−22
350	15	–	40.4	–	74	–	2.64	–	1.82	–	−24
365	15	–	34.9[e]	–	64	–	2.08	–	1.91	–	−33
200	20	–	–	–	–	–	–	–	–	–	–
215	20	16.0	29.1	29	53	0.82	1.46	0.86	1.37	−10	21
230	20	37.8	52.0[d]	69	95	2.17	4.39	0.94	1.52	−18	6
245	20	42.5	52.3[d]	77	95	2.49	4.32	1.01	1.65	−25	−7
260	20	32.3	53.3[d]	59	97	1.98	4.39	1.07	1.77	−31	−19
275	20	26.9	53.2[c]	49	97	1.56	4.32	1.12	1.75	−36	−17
290	20	22.2	52.2	40	95	1.26	4.17	1.14	1.69	−38	−11
305	20	–	42.7	–	78	–	2.76	–	1.82	–	−24
320	20	–	38.3	–	70	–	2.39	–	1.82	–	−24
335	20	–	39.8	–	73	–	2.51	–	1.93	–	−35
350	20	–	34.9[e]	–	64	–	2.12	–	1.88	–	−30
365	20	–	31.6[e]	–	58	–	1.83	–	1.92	–	−34

[a] Based on a resin strength of $\sigma_0 = 54.8$ MPa.
[b] $\varepsilon_0 = 4.12\%$.
[c] Specimen started to yield outside the weld zone and then broke at the weld.
[d] Specimen yielded and broke away from the weld zone, or tripped the limit switches set for large strains.
[e] Specimen started to sag during the joining phase.

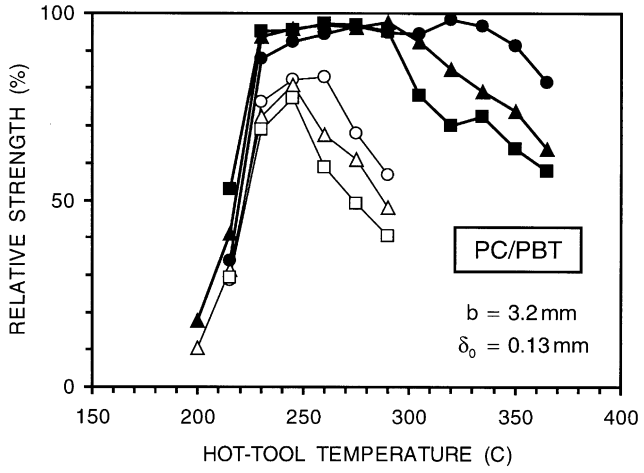

Fig. 5. Weld strength of 3.2 mm-thick PC/PBT as a function of the hot-tool temperature, with the heating time as parameter. Circles, triangles and squares correspond, respectively, to heating times of 10, 15 and 20 s. Open symbols (connected by thin lines) and solid symbols (connected by thick lines) correspond to weld penetrations of 0.25 and 0.66 mm, respectively. The melt penetration was maintained at 0.13 mm and the seal time was 10 s.

6. Weld strength of PC/PBT (Xenoy 1102)

Welds of 3.2 mm-thick PC/PBT specimens, which had a yield strength of 54.8 MPa and a yield strain of 4.12%, were made at the following conditions: Hot-tool temperatures from $T_H = 200$ to 365°C, heating times of $t_H = 10$, 15 and 20 s, a melt penetration of $\delta_0 = 0.13$ mm, two weld penetrations of $\delta_H = 0.25$ and 0.66 mm and a seal time of $t_w = 10$ s. Strength and ductility data at a nominal strain rate of 0.01 s^{-1}, and differential penetration data for welds made at these conditions, are listed in Table 3. In this table, columns 5 and 6 list, respectively, the relative weld strengths (weld strength/strength of PC/PBT resin), based on a PC/PBT resin strength of 54.8 MPa, obtained at weld penetrations of 0.25 and 0.66 mm.

The open symbols in Fig. 5, connected by thin lines, show the relative weld strength (data from Table 3) for a weld penetration of 0.25 mm as a function of the hot-tool temperature in the temperature range of $T_H = 200$–290°C, for three heating times of 10, 15 and 20 s (indicated, respectively, by the open circles, triangles and squares). For this weld penetration, the highest relative weld strength of 82–83% with a failure strain of 2.9% is obtained for $T_H =$ 245–260°C and $t_H = 10$ s. The strengths obtained for $t_H =$ 15 and 20 s are lower. Relative weld strengths in the range of 76–83% can be obtained over a narrow temperature range of 230–260°C. The fracture surfaces of all the specimens welded at $T_H \geq 230$°C were white. Specimens with low strength tended to have more bubbles in the weld zone. For $T_H \leq 230$°C, the fracture surfaces tended to have dark spots — most likely debris picked up from the hot-tool surfaces.

The filled symbols in Fig. 5, connected by thick lines, show the weld strength (data from Table 3) for the higher weld penetration of 0.66 mm as a function the hot-tool temperature for three heating times of 10, 15 and 20 s (indicated, respectively, by the filled circles, triangles and squares). Clearly, very high relative weld strengths, on the order of 98%, with failure strains of about 4.7% ($T_H = 320$°C, $t_H = 10$ s; $T_H = 290$°C, $t_H = 15$ s), can be obtained at this higher weld penetration. The weld processing window is large. Relative weld strengths greater than 91%, with failure strains larger than 3.5% can be obtained over $T_H = 245$–350°C for $t_H = 10$ s, over $T_H = 230$–305°C for $t_H = 15$ s and over $T_H = 230$–290°C for $t_H = 20$ s. Here again, the fracture surfaces of all the specimens were white, and specimens with low weld strength tended to have more bubbles in the weld zone.

6.1. Comparison with vibration welds

The vibration welding of a different batch of this is discussed in Ref. [8], where relative weld strengths of 100% with failure strains on the order of 10% have been demonstrated for 6.35 mm-thick material that had a tensile strength of 50.1 MPa. Note that this material strength and the corresponding weld strength were obtained at a lower strain rate of 0.0025 s^{-1}. The differences in resin strength, strain rates used in the tests, and specimen thickness must be considered when comparing the strengths of vibration welds with the maximum strength of about 98% achieved in hot-tool welds. Note that the highest hot-tool weld failure strains of about 4.5% are significantly lower than the 10% number demonstrated for vibration welds.

7. Weld strength of M-PPO (Noryl EM6100)

Welds of 3.2 mm-thick M-PPO specimens, which had a yield strength of 31.7 MPa and a yield strain of 2.37%, were made at the following conditions: Hot-tool temperatures from $T_H = 200$ to 365°C, heating times of $t_H = 10$, 15 and 20 s, a melt penetration of $\delta_0 = 0.13$ mm, three weld penetrations of $\delta_H = 0.25$, 0.66 and 0.91 mm and a seal time of $t_w = 10$ s. Strength and ductility data at a nominal strain rate of 0.01 s^{-1}, and length change (Δl) data for welds made at these conditions, are listed in Table 4. In this table, columns 6, 7 and 8 list, respectively, the relative weld strengths (weld strength/strength of M-PPO resin) obtained at weld penetrations of 0.25, 0.66 and 0.91 mm.

Fig. 6 shows the variations of the relative weld strength (data from Table 4) with the hot-tool temperature, for $\delta_H =$ 0.25, 0.66 and 0.91 mm. In this figure, circles, triangles and squares correspond, respectively, to heating times of 10, 15 and 20 s. The filled symbols connected by thin dashed lines correspond to $\delta_H = 0.25$ mm; the open symbols connected by thin lines correspond to $\delta_H = 0.66$ mm; the filled symbols connected by thick lines correspond to $\delta_H =$ 0.91 mm. The weld strengths for $\delta_H = 0.25$ mm are much lower than for the other two weld penetrations for all weld

Table 4
Strength and ductility data for hot-tool welds of 3.2 mm-thick M-PPO (Noryl EM6100) specimens, at a strain rate of $\dot{\varepsilon} = 0.01\ s^{-1}$, as functions of the hot-tool temperature and the heating time, for three weld penetrations of 0.25, 0.66 and 0.91 mm. The melt penetration was maintained at 0.13 mm, and the seal time was kept constant at 10 s

Hot-tool temperature (°C)	Heating time (s)	Weld strength (MPa)			Relative weld strength[a] (%)			Failure strain[b] (%)			Δl (mm)		
		$\delta_H = 0.25$ mm	$\delta_H = 0.66$ mm	$\delta_H = 0.91$ mm	$\delta_H = 0.25$ mm	$\delta_H = 0.66$ mm	$\delta_H = 0.91$ mm	$\delta_H = 0.25$ mm	$\delta_H = 0.66$ mm	$\delta_H = 0.91$ mm	$\delta_H = 0.25$ mm	$\delta_H = 0.66$ mm	$\delta_H = 0.91$ mm
200	10	[c]	[c]	–	0	0	–	[c]	[c]	–	0.76		–
215	10	[c]	[c]	–	0	0	–	[c]	[c]	–	0.84		–
230	10	6.7	12.6	–	21	40	–	0.36	0.63	–	0.91	1.49	–
245	10	8.3	16.2	–	26	51	–	0.42	0.88	–	0.96	1.59	–
260	10	14.2	18.7[d]	13.6	45	59	43	0.83	1.44	0.76	0.94	1.57	1.88
275	10	12.4	21.1[d]	14.8	39	66	47	0.71	1.54	1.07	0.97	1.66	2.05
290	10	11.9	19.4[d]	15.3	38	61	48	0.67	1.44	1.03	1.04	1.74	2.08
305	10	12.1	25.4[d]	16.3	38	80	52	0.82	2.00	1.04	1.07	1.77	2.18
320	10	–	24.6[d]	21.0	–	78	66	–	1.73	1.59	–	1.71	2.18
335	10	–	20.8[d]	23.4	–	66	74	–	1.34	1.42	–	1.79	2.22
350	10	–	24.3[d]	22.9	–	77	72	–	1.68	1.59	–	1.75	2.17
365	10	–	22.8[d]	23.3	–	72	73	–	1.46	1.54	–	1.80	2.14
200	15	[c]	[c]	–	0	0	–	[c]	[c]	–	0.80		–
215	15	8.3	11.2	–	26	35	–	0.41	0.63	–	0.85	1.64	–
230	15	6.6	16.3	–	21	52	–	0.34	0.93	–	0.93	1.66	–
245	15	9.7	19.5[d]	–	31	62	–	0.51	1.27	–	0.98	1.64	–
260	15	7.5	19.5[d]	17.1	24	61	54	0.39	1.46	1.22	1.00	1.70	2.06
275	15	11.7	22.0[d]	20.3	37	69	64	0.69	1.66	1.51	0.95	1.70	2.16
290	15	8.9	25.2[d]	18.4	28	80	58	0.50	1.83	1.35	1.06	1.77	2.18
305	15	7.5	23.5[d]	19.3	24	74	61	0.41	1.46	1.26	1.12	1.78	2.18
320	15	–	17.7[d]	21.5	–	56	68	–	1.03	1.42	–	1.70	2.15
335	15	–	18.3[d]	21.2	–	58	67	–	1.15	1.49	–	1.77	2.21
350	15	–	12.9[d]	21.8	–	41	69	–	0.68	1.56	–	1.80	2.26
365	15	–	19.6[d]	19.7	–	62	62	–	1.17	1.39	–	1.84	2.27
200	20	[c]	9.8	–	0	31	–	[c]	0.51	–	0.89	1.50	–
215	20	6.9	14.3	–	22	45	–	0.38	0.81	–	0.92	1.64	–
230	20	7.2	19.4	–	23	61	–	0.36	1.20	–	0.97	1.64	–
245	20	11.4	20.9[d]	–	36	66	–	0.61	1.29	–	0.99	1.66	–
260	20	9.2	22.4[d]	18.8	29	71	59	0.51	1.51	1.46	0.97	1.69	2.14
275	20	11.8	24.1[d]	18.2	37	76	57	0.74	1.83	1.44	0.95	1.68	2.18
290	20	9.3	23.4[d]	20.0	29	74	63	0.53	1.76	1.48	1.10	1.74	2.17
305	20	8.8	21.1[d]	21.7	28	67	69	0.49	1.27	1.52	1.13	1.79	2.12
320	20	–	18.1[d]	20.7	–	57	65	–	1.10	1.29	–	1.78	2.21
335	20	–	16.5[d]	20.2	–	52	64	–	0.90	–	–	1.83	2.18
350	20	–	13.1[d]	19.9	–	41	63	–	0.68	1.37	–	1.80	2.30
365	20	–	14.6[d]	19.3	–	46	61	–	0.88	1.20	–	1.87	2.33

[a] Based on a resin strength of $\sigma_0 = 31.7$ MPa.
[b] $\varepsilon_0 = 2.37\%$.
[c] Specimen broke while routing.
[d] Specimen had voids in the weld interface.

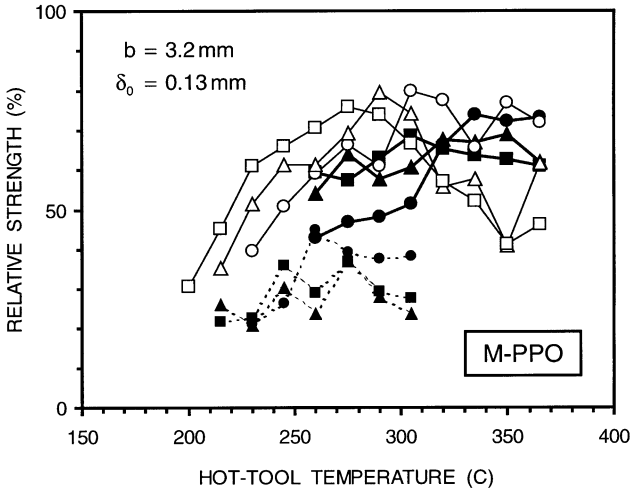

Fig. 6. Weld strength of 3.2 mm-thick M-PPO as a function of the hot-tool temperature, with the heating time as parameter. Circles, triangles and squares correspond, respectively, to heating times of 10, 15 and 20 s. Filled symbols (connected by thin dashed lines) correspond to a weld penetration of 0.25 mm. Open symbols (connected by thin lines) and solid symbols (connected by thick lines) correspond, respectively, to weld penetrations of 0.66 and 0.91 mm. The melt penetration was maintained at 0.13 mm and the seal time was 10 s.

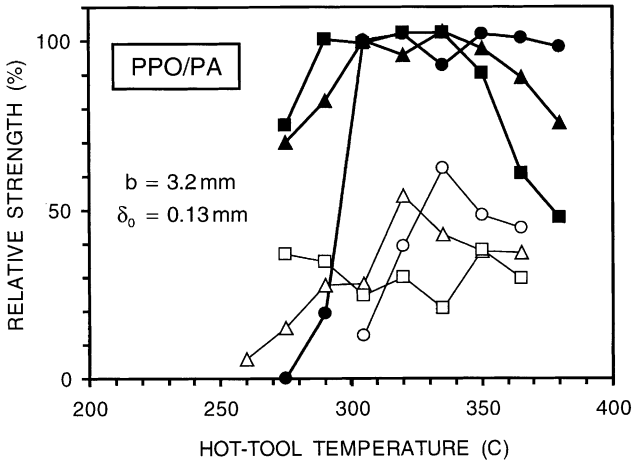

Fig. 7. Weld strength of 3.2 mm-thick PPO/PA as a function of the hot-tool temperature, with the heating time as parameter. Circles, triangles and squares correspond, respectively, to heating times of 10, 15 and 20 s. Open symbols (connected by thin lines) and solid symbols (connected by thick lines) correspond to weld penetrations of 0.25 and 0.66 mm, respectively. The melt penetration was maintained at 0.13 mm and the seal time was 10 s.

temperatures and heating times. Also, in comparison to $\delta_H = 0.91$ mm, the weld strengths are systematically higher for $\delta_H = 0.66$ mm except for $T_H = 335$–$365°C$, $t_H = 10$ s; $T_H = 320$–$365°C$, $t_H = 15$ s; $T_H = 305$–$365°C$, $t_H = 20$ s. The highest strengths are obtained for $\delta_H = 0.66$ mm, for which relative weld strengths of about 80%, with failure strains of about 2% can be obtained ($T_H = 305°C$, $t_H = 10$ s; $T_H = 290°C$, $t_H = 15$ s). Note that for this material, $\Delta\eta > 0$ for all the welds, indicating that the molten material at the weld interface solidified under pressure.

8. Weld strength of PPO/PA (Noryl GTX 910)

Welds of 3.2 mm-thick PPO/PA specimens, having a yield strength of 54.0 MPa and a yield strain of 11.1%, were made at the following conditions: Hot-tool temperatures from $T_H = 260$ to $380°C$, heating times of $t_H = 10$, 15 and 20 s, a melt penetration of $\delta_0 = 0.13$ mm, two weld penetrations of $\delta_H = 0.25$ and 0.66 mm and a seal time of $t_w = 10$ s. Strength and ductility data at a nominal strain rate of 0.01 s^{-1}, and differential penetration data for welds made at these conditions, are listed in Table 5. In this table, columns 5 and 6 list, respectively, the relative weld strengths (weld strength/strength of PPO/PA resin), based on a PPO/PA resin strength of 54.0 MPa, obtained at weld penetrations of 0.25 and 0.66 mm.

Fig. 7 shows the variations of the relative weld strength (data from Table 5) with the hot-tool temperature, for $\delta_H = 0.25$ and 0.66 mm. In this figure, circles, triangles and squares correspond, respectively, to heating times of 10, 15 and 20 s. The open symbols connected by thin lines correspond to $\delta_H = 0.25$ mm and the filled symbols connected by thick lines correspond to $\delta_H = 0.66$ mm. Clearly, very high relative weld strengths, on the order of 100%, can be obtained at the higher weld penetration of 0.66 mm. For $t_H = 10$ s, except at $T_H = 335°C$ at which $\sigma_R = 93\%$, $\sigma_R \geq 100\%$ for $T_H = 305$–$365°C$ and the corresponding failure strains are about 6.3%. For $t_H = 15$ s, $\sigma_R \geq 100\%$ at $T_H = 305$ and $335°C$ — even at $T_H = 320$ and $350°C$, $\sigma_R = 96$ and 98%, respectively. And for $t_H = 20$ s, except at $T_H = 305°C$ at which $\sigma_R = 99\%$, $\sigma_R \geq 100\%$ for $T_H = 290$–$335°C$, and the corresponding failure strains are in the range of 4.6–8%. Note that at these process conditions, the differential penetration (last column in Table 5) is positive indicating that the stops do not contact during the joining phase, so that the weld interface solidifies under pressure. Some of the very high weld strength may be explained by increases in the weld interface area caused by the weld pressure during the joining phase. Note also that the molten interface tended to smoke for $T_H \geq 305°C$. The fracture surfaces of the strongest welds had a rough texture and, in some cases, some white streaks. Welds made at the very high temperatures had very crusty fracture surfaces.

The weld strengths obtained at the lower penetration of 0.25 mm are much lower with a maximum relative weld strength of 62%. For this weld penetration, the molten interface tended to smoke for $T_H \geq 320°C$. And the fracture surfaces of all the welds made with $T_H \geq 275°C$ showed remnants of tiny bubbles.

9. Weld strength of 30GF-MPPO (Noryl GFN3)

Welds of 3.2 mm-thick 30GF-MPPO specimens had a

Table 5
Strength and ductility data for hot-tool welds of 3.2 mm-thick PPO/PA (Noryl GTX 910) specimens, at a strain rate of $\dot{\varepsilon} = 0.01\ s^{-1}$, as functions of the hot-tool temperature and the heating time, for two weld penetrations of 0.25 and 0.66 mm. The melt penetration was maintained at 0.13 mm

Hot-tool temperature (°C)	Heating time (s)	Weld strength (MPa)		Relative weld strength[a] (%)		Failure strain[b] (%)		Δl (mm)		Differential penetration $\Delta\eta$ (10^{-2} mm)	
		$\delta_H = 0.25$ mm	$\delta_H = 0.66$ mm	$\delta_H = 0.25$ mm	$\delta_H = 0.66$ mm	$\delta_H = 0.25$ mm	$\delta_H = 0.66$ mm	$\delta_H = 0.25$ mm	$\delta_H = 0.66$ mm	$\delta_H = 0.25$ mm	$\delta_H = 0.66$ mm
260	10	[c]	–	–	–	–	–	–	–	–	–
275	10	[c]	[d]	–	–	–	–	–	–	–	–
290	10	[d]	10.4	–	19	–	0.45	–	0.79	–	79
305	10	6.9	53.9	13	100	0.33	4.70	0.94	0.96	−18	62
320	10	21.2	54.9	39	102	1.19	6.25	1.09	1.12	−33	46
335	10	33.6	50.0	62	93	2.26	3.70	1.13	1.20	−37	38
350	10	26.1	55.1	48	102	1.53	6.28	1.12	1.30	−36	28
365	10	24.2	54.5	45	101	1.46	6.41	1.17	1.52	−41	6
380	10	–	53.0	–	98	–	4.97	–	1.62	–	−4
260	15	3.0	–	6	–	0.12	–	0.80	–	−4	–
275	15	8.1	37.9	15	70	0.43	2.11	0.91	0.79	−15	79
290	15	14.9	44.4	28	82	0.82	2.78	0.99	0.96	−23	62
305	15	15.2	53.9	28	100	0.92	5.47	1.05	1.14	−29	44
320	15	29.2	51.7	54	96	1.79	4.08	1.18	1.38	−42	20
335	15	23.1	55.4	43	103	1.35	9.14	1.17	1.45	−41	13
350	15	20.3	52.8	38	98	1.16	4.64	1.19	1.51	−43	7
365	15	20.1	48.2	37	89	1.18	3.32	1.19	1.69	−43	−11
380	15	–	41.0	–	76	–	2.45	–	1.77	–	−19
260	20	[d]	–	–	–	–	–	–	–	–	–
275	20	20.0	40.5	37	75	1.17	2.33	0.94	0.93	−18	65
290	20	18.8	54.3	35	100	1.02	4.58	1.04	1.09	−28	49
305	20	13.3	53.7	25	99	0.74	5.01	1.14	1.27	−38	31
320	20	16.3	55.3	30	102	0.89	6.46	1.13	1.52	−37	6
335	20	11.3	55.2	21	102	0.68	8.05	1.17	1.59	−41	−1
350	20	20.5	48.8	38	90	1.33	3.23	1.21	1.69	−45	−11
365	20	16.0	32.8	30	61	0.96	1.93	1.24	1.74	−48	−16
380	20	–	25.7	–	48	–	1.57	–	1.75	–	−17

[a] Based on a resin strength of $\sigma_0 = 54.0$ MPa.
[b] $\varepsilon_0 = 11.1\%$.
[c] Welded specimen broke before routing.
[d] Welded specimen broke during routing.

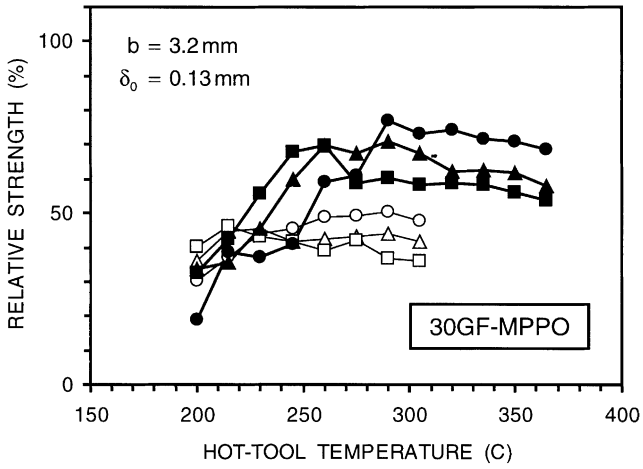

Fig. 8. Weld strength of 3.2 mm-thick 30GF-MPPO as a function of the hot-tool temperature, with the heating time as parameter. Circles, triangles and squares correspond, respectively, to heating times of 10, 15 and 20 s. Open symbols (connected by thin lines) and solid symbols (connected by thick lines) correspond to weld penetrations of 0.25 and 0.66 mm, respectively. The melt penetration was maintained at 0.13 mm and the seal time was 10 s.

yield strength of 80.1 MPa and a yield strain of 1.78%, were made at the following conditions: Hot-tool temperatures from $T_H = 260$ to 280°C, heating times of $t_H = 10$, 15 and 20 s, a melt penetration of $\delta_0 = 0.13$ mm, two weld penetrations of $\delta_H = 0.25$ and 0.66 mm and a seal time of $t_w = 10$ s. Strength and ductility data at a nominal strain rate of 0.01 s^{-1}, and differential penetration data for welds made at these conditions, are listed in Table 6. In this table, columns 5 and 6 list, respectively, the relative weld strengths (weld strength/strength of PPO/PA resin), based on a PPO/PA resin strength of 54.0 MPa, obtained at weld penetrations of 0.25 and 0.66 mm.

Fig. 8 shows the variations of the relative weld strength (data from Table 6) with the hot-tool temperature, for $\delta_H = 0.25$ and 0.66 mm. In this figure, circles, triangles and squares correspond, respectively, to heating times of 10, 15 and 20 s. The open symbols connected by thin lines and the filled symbols connected by thick lines correspond, respectively, to $\delta_H = 0.25$ and 0.66 mm. Clearly, higher weld strengths are obtained at the higher weld penetration of 0.66 mm. And, at this penetration, the relative weld strengths are highest for $t_H = 10$ s, with a maximum of about 77% at $T_H = 290$°C. For $t_H = 10$ s, the relative weld strengths in the range of 71–77% can be obtained in the large temperature range of $T_H = 290$–350°C. The corresponding failure strains vary in the range of 1.1–1.3%. With a maximum of 51% ($T_H = 290$°C, $t_H = 10$ s), the attainable relative weld strengths at the lower weld penetration of 0.25 mm are substantially lower than 0.66 mm. The failure strains are also lower, being less than 0.7%. While the attainable relative weld strengths are not very high, the hot-tool temperature process window over which high strengths can be obtained is fairly large. This is consistent with what has been observed in the hot-tool welding of 30% glass-filled PBT [2], in which, while relative weld strength attained is much lower (≈ 0.5) than that of the unfilled material (≈ 1), consistent weld strength can be obtained in the glass-filled material over a much wider weld process window.

At the lower weld penetrations, the fracture surfaces had bubbles, the numbers of which increase with the hot-tool temperature. Also, for $T_H \geq 200$°C, the material tended to smoke during the changeover phase.

9.1. Comparison with vibration welds

Data on vibration welding of this material are not available. However, some idea about how glass fibers affect weld strength can be had from vibration welding data available for two glass-filled resins. Relative strengths on the order of 65 and 55% have been demonstrated in vibration welds of 6.1 mm-thick specimens of 15 and 30 wt% glass-filled PBT, 15GF-PBT (VALOX DR51) and 30GF-PBT (VALOX 420), respectively [4]. And relative strengths on the order of 45 and 70% have been demonstrated in vibration welds of 3.2 and 6.1 mm-thick specimens, respectively, of 20 wt% glass-filled M-PPO (Noryl GFN2-701) [9].

10. Weld strength of PC/ABS-2 (Cycoloy MC8002) to M-PPO (Noryl EM6100)

A limited number of tests were done to explore the weldability Cycoloy MC8002 (PC/ABS-2), which has a tensile strength of 54.6 MPa — a PC/ABS blend that is very similar to Cycoloy C2950HF — to Noryl EM6100, which has a tensile strength of 31.7 MPa.

Welds of 3.2 mm-thick PC/ABS-2 specimens with M-PPO specimens of the same thickness were made at the following conditions: Hot-tool temperatures in the range $T_H =$ 260–305°C for $\delta_H = 0.25$ mm and $T_H = 230$–335°C for $\delta_H = 0.66$ mm. Tests were done at three heating times of $t_H =$ 10, 15 and 20 s, a melt penetration of $\delta_0 = 0.13$ mm and a seal time of $t_w = 10$ s. Strength and ductility data at a nominal strain rate of 0.01 s^{-1}, and differential penetration data for welds made at these conditions, are listed in Table 7. In this table, columns 5 and 6 list, respectively, the relative weld strengths (weld strength/strength of M-PPO resin) obtained at weld penetrations of 0.25 and 0.66 mm. Note that the relative strengths are based on the tensile strength, 37.1 MPa, of M-PPO, the weaker of the two materials, which has a failure strain of 2.37%.

Fig. 9 shows the variations of the relative weld strength (data from Table 7) with the hot-tool temperature, for $\delta_H = 0.25$ and 0.66 mm. In this figure, circles, triangles and squares correspond, respectively, to heating times of 10, 15 and 20 s. The open symbols connected by thin lines and the filled symbols connected by thick lines correspond, respectively, to $\delta_H = 0.25$ and 0.66 mm. Clearly, higher weld strengths are obtained at the higher weld penetration of 0.66 mm, for which relative weld strengths of about 38%,

Table 6
Strength and ductility data for hot-tool welds of 3.2 mm-thick 30GF-MPPO (Noryl GFN3) specimens, at a strain rate of $\dot{\varepsilon} = 0.01\ s^{-1}$, as functions of the hot-tool temperature and the heating time, for two weld penetrations of 0.25 and 0.66 mm. The melt penetration was maintained at 0.13 mm

Hot-tool temperature (°C)	Heating time (s)	Weld strength (MPa)		Relative weld strength[a] (%)		Failure strain[b] (%)		Δl (mm)		Differential penetration $\Delta\eta$ (10^{-2} mm)	
		$\delta_H = 0.25$ mm	$\delta_H = 0.66$ mm	$\delta_H = 0.25$ mm	$\delta_H = 0.66$ mm	$\delta_H = 0.25$ mm	$\delta_H = 0.66$ mm	$\delta_H = 0.25$ mm	$\delta_H = 0.66$ mm	$\delta_H = 0.25$ mm	$\delta_H = 0.66$ mm
200	10	24.2	15.2	30	19	0.36	0.22	0.52	0.42	24	116
215	10	29.6	31.1	37	39	0.47	0.56	0.69	0.86	7	72
230	10	35.4	29.6	44	37	0.55	0.45	0.75	1.24	1	34
245	10	36.4	32.9	46	41	0.62	0.63	0.84	1.51	−8	7
260	10	39.1	47.5	49	59	0.62	0.95	0.81	1.61	−5	−3
275	10	39.5	49.1	49	61	0.69	1.05	0.81	1.66	−5	−8
290	10	40.5	61.8	51	77	–	1.33	0.84	1.57	−8	1
305	10	38.2	58.6	48	73	0.67	1.29	0.85	1.59	−9	−1
320	10	–	59.6	–	74	–	1.14	–	1.61	–	−3
335	10	–	57.5	–	72	–	1.22	–	1.64	–	−6
350	10	–	56.7	–	71	–	1.10	–	1.63	–	−5
365	10	–	55.0	–	69	–	1.21	–	1.66	–	−8
200	15	28.8	27.0	36	34	0.46	0.47	0.66	0.65	10	93
215	15	36.0	28.6	45	36	0.61	0.52	0.78	1.31	−2	27
230	15	36.5	36.3	46	45	0.62	0.63	0.81	1.54	−5	4
245	15	33.4	48.0	42	60	0.55	1.00	0.81	1.60	−5	−2
260	15	34.2	56.0	43	70	0.58	1.29	0.88	1.61	−12	−3
275	15	34.7	54.0	43	67	0.60	0.98	0.81	1.66	−5	−8
290	15	35.2	56.8	44	71	0.67	1.23	0.87	1.57	−11	1
305	15	33.5	54.1	42	68	0.61	1.09	0.87	1.60	−11	−2
320	15	–	50.0	–	62	–	1.10	–	1.65	–	−7
335	15	–	50.1	–	63	–	1.11	–	1.65	–	−7
350	15	–	49.6	–	62	–	1.05	–	1.63	–	−5
365	15	–	46.5	–	58	–	0.95	–	1.66	–	−8
200	20	32.2	26.1	32.2	33	–	0.43	0.75	1.03	10	55
215	20	37.1	34.0	37.1	42	0.57	0.61	0.81	1.45	−2	13
230	20	34.6	44.8	34.6	56	0.59	0.95	0.83	1.57	−5	1
245	20	33.3	54.5	33.3	68	0.55	1.07	0.84	1.61	−5	−3
260	20	31.2	55.8	31.2	70	0.56	1.12	0.83	1.65	−12	−7
275	20	33.6	47.1	33.6	59	0.57	0.90	0.86	1.65	−5	−7
290	20	29.3	48.4	29.3	60	0.53	0.98	0.86	1.64	−11	−6
305	20	28.9	46.7	28.9	58	0.53	0.94	0.87	1.66	−11	−8
320	20	–	47.2	–	59	–	0.99	–	1.61	–	−3
335	20	–	46.7	–	58	–	0.95	–	1.68	–	−10
350	20	–	45.0	–	56	–	0.97	–	1.66	–	−8
365	20	–	43.1	–	54	–	0.91	–	1.69	–	−11

[a] Based on a resin strength of $\sigma_0 = 80.1$ MPa.
[b] $\varepsilon_0 = 1.78\%$.

Table 7
Strength and ductility data for hot-tool welds of 3.2 mm-thick PC/ABS-2 (Cycoloy MC8002) to M-PPO (Noryl EM6100) specimens, at a strain rate of $\dot{\varepsilon} = 0.01\ s^{-1}$, as functions of the hot-tool temperature and the heating time, for two weld penetrations of 0.25 and 0.66 mm. The melt penetration was maintained at 0.13 mm

Hot-tool temperature (°C)	Heating time (s)	Weld strength (MPa)		Relative weld strength[a] (%)		Failure strain[b] (%)		Δl (mm)		Differential penetration $\Delta\eta$ (10^{-2} mm)	
		$\delta_H = 0.25$ mm	$\delta_H = 0.66$ mm	$\delta_H = 0.25$ mm	$\delta_H = 0.66$ mm	$\delta_H = 0.25$ mm	$\delta_H = 0.66$ mm	$\delta_H = 0.25$ mm	$\delta_H = 0.66$ mm	$\delta_H = 0.25$ mm	$\delta_H = 0.66$ mm
230	10	–	3	–	8	–	0.08	–	1.47	–	−15
245	10	–	13	–	40	–	0.58	–	1.39	–	−7
260	10	[c]	11	0	34	–	0.50	–	1.47	–	−15
275	10	[c]	12	0	38	–	0.58	–	1.51	–	−19
290	10	7.0	12	22	39	0.35	0.62	1.06	1.58	−56	−26
305	10	6.2	12	20	37	0.28	0.57	1.14	1.56	−64	−24
320	10	–	10	–	31	–	0.45	–	1.53	–	−21
335	10	–	9	–	30	–	0.43	–	1.59	–	−27
230	15	–	9	–	28	–	0.38	–	1.45	–	−13
245	15	–	11	–	35	–	0.50	–	1.48	–	−16
260	15	5.1	12	16	37	0.22	0.56	1.03	1.51	−53	−19
275	15	5.9	10	19	32	0.26	0.49	1.04	1.54	−54	−22
290	15	6.0	9	19	30	0.26	0.45	1.07	1.61	−57	−29
305	15	5.7	10	18	31	0.27	0.48	1.10	1.63	−60	−31
320	15	–	8	–	25	–	0.37	–	1.61	–	−29
335	15	–	[c]	–	–	–	–	–		–	–
230	20	–	[c]	–	–	–	–	–	–	–	–
245	20	–	8	–	24	–	0.31	–	1.50	–	−18
260	20	5.2	10	16	32	0.22	0.51	1.01	1.54	−51	−22
275	20	[c]	9	–	29	–	0.46	–	1.61	–	−29
290	20	[c]	8	–	24	–	0.38	–	1.64	–	−32
305	20	[c]	9	–	29	–	0.45	–	1.63	–	−31
320	20	–	5	–	16	–	0.23	–	1.68	–	−36
335	20	–	6	–	18	–	0.23	–	1.69	–	−37

[a] Based on an M-PPO resin strength of $\sigma_0 = 31.7$ MPa.
[b] $\varepsilon_0 = 2.37\%$.
[c] Specimen broke while routing.

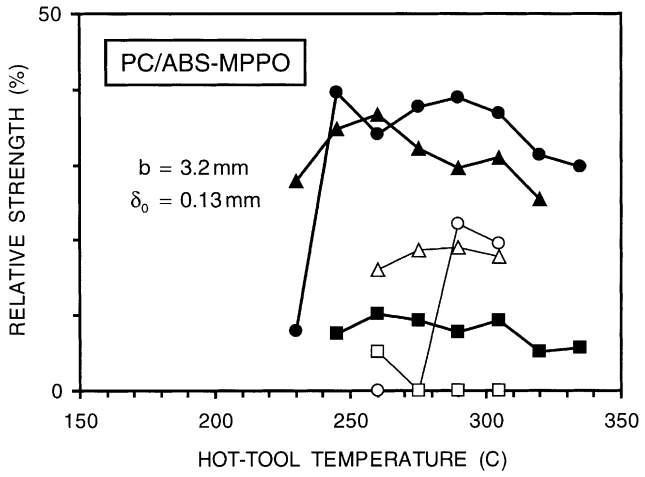

Fig. 9. Weld strength of 3.2 mm-thick PC/ABS-2 to M-PPO welds as a function of the hot-tool temperature, with the heating time as parameter. Circles, triangles and squares correspond, respectively, to heating times of 10, 15 and 20 s. Open symbols (connected by thin lines) and solid symbols (connected by thick lines) correspond to weld penetrations of 0.25 and 0.66 mm, respectively. The melt penetration was maintained at 0.13 mm and the seal time was 10 s.

with failure strains of about 0.6%, can be attained in the temperature range $T_H = 275–305°C$ with $t_H = 10$ s.

11. Concluding remarks

All of the data in this paper were obtained from one test per weld process condition studied. While such data do not provide information on repeatability, they are useful for an initial mapping of weldability over a wide range of weld process conditions. Attainable strengths in hot-tool welds of several different resins have been characterized. For some of the resins, hot-tool weld strengths have been compared with strengths of vibration welds.

In ABS (Cycolac BDT 6500), 100% relative weld strengths with strains to failure of about 2.1% can be obtained in the hot-tool temperature range $T_H =$ 230–260°C for a heating time of $t_H = 10$ s. For $t_H = 15$ s, 100% relative weld strengths can be obtained for $T_H =$ 230–245°C, with failure strains of 2.2%. Higher weld strengths are achieved at the higher weld penetration of 0.66 mm.

In PC/ABS (Cycoloy C2950HF), a maximum relative weld strength of 91%, with a failure strains of 2.6%, was demonstrated at a weld temperature of $T_H = 290°C$, at $t_H = 10$ s. Here again, higher weld strengths are achieved at the higher weld penetration of 0.66 mm.

In PC/PBT (Xenoy 1102), very high relative weld strengths, on the order of 98%, with failure strains of about 4.7% ($T_H = 320°C$, $t_H = 10$ s; $T_H = 290°C$, $t_H = 15$ s), can be obtained at a weld penetration of 0.66 mm. Relative weld strengths greater than 91%, with failure strains larger than 3.5% can be obtained over a wide weld processing window of $T_H = 245–350°C$ for $t_H = 10$ s, over $T_H = 230–305°C$ for $t_H = 15$ s, and over $T_H = 230–290°C$ for $t_H = 20$ s.

In M-PPO (Noryl EM6100), relative weld strengths of about 80% with failure strains of about 2% have been demonstrated ($T_H = 305°C$, $t_H = 10$ s; $T_H = 290°C$, $t_H = 15$ s) for a weld penetration of $\delta_H = 0.66$ mm.

PPO/PA (Noryl GTX 910) welds extremely well. For a weld penetration of 0.66 mm, very high relative weld strengths on the order of 100%, with high failure strains larger than 4%, can be obtained over a very wide weld processing window of $T_H = 305–365°C$ and $t_H = 10$ s; $T_H = 305–350°C$ and $t_H = 15$ s; $T_H = 290–335°C$ and $t_H = 20$ s.

In 30GF-MPPO (Noryl GFN3), relative weld strengths in the range of 71–77% can be obtained over the fairly large temperature window of $T_H = 290–350°C$ with $t_H = 10$ s. The corresponding failure strains vary in the range of 1.1–1.3%.

In hot-tool welds PC/ABS-2 (Cycoloy MC8002) to M-PPO (Noryl EM6100), relative weld strengths of about 38%, with failure strains of about 0.6%, have been demonstrated for $T_H = 275–305°C$ with $t_H = 10$ s.

Acknowledgements

This work was supported by GE Plastics and the NIST ATP Project: Engineering Design with Injection-Molded Thermoplastics. The contributions of L.P. Inzinna are greatly appreciated.

References

[1] Stokes VK. Polymer 1999;40:6235.
[2] Stokes VK. Polymer 2000;41:4317.
[3] Stokes VK. Polymer 2001;42:775.
[4] Stokes VK. Polymer 1993;34:4445.
[5] Stokes VK. Polym Engng Sci 1988;28:998.
[6] Stokes VK. Polym Engng Sci 1997;37:692.
[7] Stokes VK. Polym Engng Sci 2000;40:2175.
[8] Stokes VK. Polymer 1992;33:1237.
[9] Stokes VK. Polym Engng Sci 1991;31:511.